$Et_4N[Mo_2(CO)_{10}H]$. This binuclear anion resonates (Table I, Figure 4) at high field as expected for a formally Mo(0) species. ^{95}Mo–^{1}H coupling, $^1J(^{95}Mo,^1H) = 15$ Hz, is observed directly and was confirmed by proton decoupling.

***trans*-$[Mo(N_2)_2(dptpe)_2]$ and Related Species.** It was necessary to heat these systems above room temperature in order to detect resonances under the present conditions. The observation (Table II, Figure 1d) of a quintet for *trans*-$[Mo(N_2)_2(dptpe)_2]$ in tetrahydrofuran (THF) under dinitrogen at 55 °C confirms a trans configuration with four equivalent phosphorus atoms. The integrity of the solution was monitored by infrared spectroscopy[25] at room temperature before and after the measurement. In addition, ^{15}N NMR measurements[31] confirm the stability of $[Mo(N_2)_2(PR_3)_4]$ species in THF under argon at 30 °C. The ^{95}Mo chemical shift of −776 ppm for this compound is the lowest field signal yet observed for a formally Mo(0) species and further illustrates the large deshielding effect of nitrogen donors. Interestingly, $^1J(^{95}Mo,^{31}P)$, 205 Hz, is larger than expected on the basis of comparisons with the other systems studied. The chemical shift range for Mo(0) is now −776 to −2200 ppm, and an extension to lower field can be expected as more nitrogen-containing species are examined. Examination of the chemical shift ranges presented in the Introduction make it apparent that the ^{95}Mo chemical shift cannot be used to distinguish among mononuclear species of Mo(0), Mo(II), and Mo(IV). However, the shift is highly sensitive to structural and electronic variations within a closely related series of mononuclear compounds, as illustrated in previous work[4,5,9] and in Table I.

A solution obtained by treating *trans*-$[Mo(N_2)_2(dptpe)_2]$ in THF with CO for 24 h showed two incompletely resolved multiplets at −1802 and −1475 ppm, which suggest the presence of *cis*- and *trans*-$[Mo(CO)_2(dptpe)_2]$. The tetrahydride $[MoH_4(dptpe)]$ in toluene at 65 °C exhibited a broad resonance at −1805 ppm: ^{95}Mo–^{1}H and ^{95}Mo–^{31}P coupling was not observed, almost certainly due to intramolecular exchange processes which have been observed with such species by ^{1}H NMR.[25]

Acknowledgment. We thank Professors J. H. Enemark, G. P. Haight, Jr., G. C. Levy, and E. Oldfield for preprints of results. The Australian Research Grants Scheme and the Australian Wool Corp. are thanked for generous support of this work.

Registry No. ^{95}Mo, 14392-17-7; $[Mo(CO)_6]$, 13939-06-5; $Na[HMo_2(CO)_{10}]$, 84417-20-9; $[Mo(CO)_5(PEt_3)]$, 19217-79-9; $[Mo(CO)_5(P(n\text{-}Bu)_3)]$, 15680-62-3; $[Mo(CO)_5(PPh_3)]$, 14971-42-7; $[Mo(CO)_5(AsPh_3)]$, 19212-22-7; $[Mo(CO)_5(SbPh_3)]$, 19212-21-6; $[Mo(CO)_5(PMe_2Ph)]$, 24554-78-7; $[Mo(CO)_5(PEt_2Ph)]$, 72868-87-2; $[Mo(CO)_5(P(n\text{-}Bu)_2Ph)]$, 18534-33-3; $[Mo(CO)_5(P(OMe)_3)]$, 15631-20-6; $[Mo(CO)_5(P(OEt)_3)]$, 15603-75-5; $[Mo(CO)_5(P(OPr\text{-}i)_3)]$, 34369-19-2; $[Mo(CO)_5(P(OBu\text{-}n)_3)]$, 21485-22-3; $[Mo(CO)_5(P(OPh)_3)]$, 15711-66-7; $[Mo(CO)_4(bpy)]$, 15668-64-1; *cis*-$[Mo(CO)_4(PEt_3)_2]$, 19217-80-2; *cis*-$[Mo(CO)_4(P(n\text{-}Bu)_3)_2]$, 16244-54-5; *cis*-$[Mo(CO)_4(P(n\text{-}Bu)_2Ph)_2]$, 29825-19-2; *cis*-$[Mo(CO)_4(Ph_2PCH_2PPh_2)]$, 26743-81-7; *cis*-$[Mo(CO)_4(Ph_2P(CH_2)_2PPh_2)]$, 15444-66-3; *cis*-$[Mo(CO)_4(Ph_2P(CH_2)_3PPh_2)]$, 15553-68-1; *cis*-$[Mo(CO)_4(P(OMe)_3)_2]$, 15631-22-8; *cis*-$[Mo(CO)_4(P(OEt)_3)_2]$, 38604-20-5; *cis*-$[Mo(CO)_4(P(OPr\text{-}i)_3)_2]$, 84472-14-0; *cis*-$[Mo(CO)_4(P(OBu\text{-}n)_3)_2]$, 84472-15-1; *cis*-$[Mo(CO)_4(P(OPh)_3)_2]$, 59599-01-8; *fac*-$[Mo(CO)_3(P(Bu\text{-}n)_3)_3]$, 29825-20-5; *fac*-$[Mo(CO)_3(P(OMe)_3)_3]$, 15631-24-0; *fac*-$[Mo(CO)_3(P(OEt)_3)_3]$, 38542-39-1; *fac*-$[Mo(CO)_3(bpy)(P(OEt)_3)]$, 84472-16-2; *trans*-$[Mo(N_2)_2(dptpe)_2]$, 70320-87-5; $[MoH_4(dptpe)_2]$, 70320-86-4; $[Mo(CO)_2(dptpe)_2]$, 84417-21-0.

---

(31) Chatt, J.; Fakley, M. E.; Richards, R. L.; Mason, J.; Stenhouse, I. A. *J. Chem. Res., Synop.* **1979**, 44.

Contribution from the Department of Chemistry,
University of Nottingham, Nottingham, England NG7 2RD

Mixed Carbonyl–Dinitrogen Compounds: Synthesis and Thermal Stability of $Cr(CO)_{6-x}(N_2)_x$ in Liquid-Xenon Solution and Low-Temperature Matrices

JAMES J. TURNER,* MICHAEL B. SIMPSON, MARTYN POLIAKOFF, WILLIAM B. MAIER II,[1a]
and MICHAEL A. GRAHAM[1b]

Received April 14, 1982

The mixed carbonyl–dinitrogen species of Cr, $Cr(CO)_{6-x}(N_2)_x$ ($x = 1$–5), have been generated by UV photolysis of $Cr(CO)_6$ in liquid Xe/N_2 mixtures, at 183 K. The product species are identified by IR spectroscopy and characterized on the basis of photochemical behavior, and thermal stability, by comparison with simple theoretical arguments of predicted IR band intensity and position. Further detailed identification is also achieved by selective narrow-band photolysis at 367 nm, which distinguishes between cis/trans and *mer*/*fac* isomers of $Cr(CO)_4(N_2)_2$ and $Cr(CO)_3(N_2)_3$, respectively. Comparison is also made with matrix isolation experiments, including isotopic ($C^{18}O$) substitution. The molecule $Cr(CO)_5N_2$ is found to be thermally stable in solution in liquid xenon at −35 °C, whereas the most highly N_2-substituted species $Cr(CO)(N_2)_5$ is thermally unstable at −90 °C.

I. Introduction

The matrix isolation technique has proved extremely valuable for the structural characterization of coordinatively *unsaturated* species such as $Cr(CO)_5$[2] and $Fe(CO)_4$.[3] It has also, however, proved its value in characterizing unstable coordinatively *saturated* species such as $Ni(N_2)_4$,[4] $Pd(CO)_4$,[5] and $Ni(CO)_3N_2$.[6,7] Recently, we have shown[8] that some of these saturated species may be spectroscopically examined following photochemical generation using *liquid* noble-gas

---

(1) (a) Present address: Los Alamos National Laboratory, Los Alamos, NM 87545. (b) Present address: Perkins Engines Ltd., Eastfield, Peterborough, UK.

(2) (a) Graham, M. A.; Poliakoff, M.; Turner, J. J. *J. Chem. Soc. A* **1971**, 2939–2948. (b) Perutz, R. N.; Turner, J. J. *Inorg. Chem.* **1975**, *14*, 262–270.

(3) Poliakoff, M.; Turner, J. J. *J. Chem. Soc., Dalton Trans.* **1974**, 2276–2285.

(4) Huber, H.; Kundig, E. P.; Moskovits, M.; Ozin, G. A. *J. Am. Chem. Soc.* **1973**, *95*, 332.

(5) Darling, J. H.; Ogden, J. S. *Inorg. Chem.* **1972**, *11*, 666.

(6) Kundig, E. P.; Moskovits, M.; Ozin, G. A. *Can. J. Chem.* **1973**, *51*, 2737.

(7) Rest, A. J. *J .Organomet. Chem.* **1972**, *40*, C76.

(8) (a) Maier II, W. B.; Poliakoff, M.; Simpson, M. B.; Turner, J. J. *J. Chem. Soc., Chem. Commun.* **1980**, 587. (b) Maier II, W. B.; Poliakoff, M.; Simpson, M. B.; Turner, J. J. *J. Mol. Struct.* **1982**, *80*, 83.

0020-1669/83/1322-0911$01.50/0

solvents. Our noble-gas technique is complementary to the recently developed low-temperature hydrocarbon and liquid polymer techniques.[9] This paper is concerned with the preparation of the species $Cr(CO)_{6-x}(N_2)_x$ ($x = 1-5$), where the absence of IR bands due to the noble-gas solvent is a distinct advantage.

Previous studies on $M/CO/N_2$ complexes have employed the matrix technique in two ways. The first approach is the cocondensation of a stream of metal atoms onto a cold window (typically 10 K) with a stream of CO and/or N_2, producing species that can be characterized by IR, Raman, and occasionally ESR spectroscopy; for example, Cr + N_2 gives $Cr(N_2)_6$[10] and V + CO gives $V(CO)_6$,[11] but of particular relevance for this paper is the production of $Ni(CO)_{4-x}(N_2)_x$ by cocondensation[6] of Ni + CO/N_2. Alternatively, UV photolysis of a stable parent compound, already trapped in N_2-doped matrices, may produce substituted species; for example, $Ni(CO)_4$ in N_2 gives[7] $Ni(CO)_3N_2$, and $M(CO)_6$ (M = Cr, Mo, W) in N_2 gives $M(CO)_5N_2$ and evidence for further substitution.[12]

In both types of matrix experiments there is the ubiquitous problem of "site splittings"; these arise because isolated molecules may find themselves in a number of slightly different environments in the solid host, and the resulting IR bands are often split. This is a particularly serious problem when there are several different species in the matrix, since it is sometimes impossible to distinguish matrix splittings from genuine spectral differences due to different molecules. A further disadvantage of matrix isolation is the inability to make a proper study of thermal stability—it is not always easy to distinguish between spectral changes brought about by "softening" a matrix on heating and those due to changes in the stability of trapped molecules with temperature. Noble gases as solvents promise to overcome both of these difficulties, and we have previously demonstrated[8] the quality of IR data that can be obtained for $Cr(CO)_5N_2$, generated by photolysis of $Cr(CO)_6$ in liquid xenon at −78 °C containing a trace of N_2. Further photolysis of this system in the presence of an increased concentration of N_2 produces further substitution of CO by N_2.

In this paper, we describe experiments to characterize the species $Cr(CO)_{6-x}(N_2)_x$. Because of the large number of possible species in this case (much greater than for $Ni(CO)_{4-x}(N_2)_x$), we have only been able to solve the problem by a combination of all three methods, noble-gas solution photochemistry, matrix isolation cocondensation, and matrix photochemistry. In fact, the matrix work was done some years ago[13] and a full interpretation has only become possible with the advent of our liquid-Xe work. Finally, we wish to emphasize the value of Timney's[14] approximate force field method in helping to unravel this complex system.

The paper starts with a description of the *liquid*-Xe experiments and shows how a large part of the problem of identification is solved by this novel technique when combined with approximate intensity and force field arguments.

II. Experimental Section

Matrix Isolation Experiments. These were all performed at the University Chemical Laboratories, Cambridge University, and the experimental details are given very fully elsewhere.[13] The apparatus consisted of an Air Products AC-2L "Cryotip" Joule Thomson Liquefier and a Perkin-Elmer 521 IR spectrometer. Cr atoms were generated by resistive heating of Cr metal foil. All gases were BOC grade X (including Xe for the liquid experiments below).

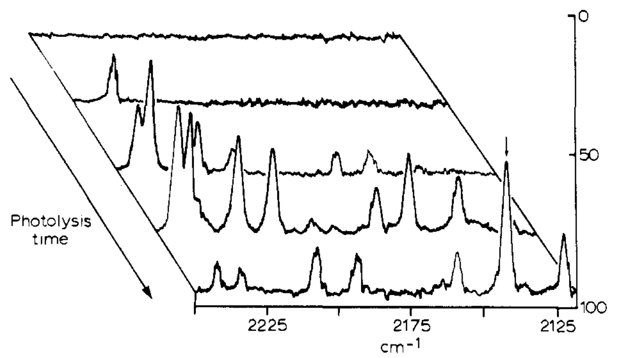

Figure 1. IR spectrum of a solution containing $Cr(CO)_6$ dissolved in a liquid Xe/N_2 mixture in the NN stretching region 2300–2120 cm^{-1}. The successive spectra have been recorded after progressively lengthier periods of photolysis. No absorptions are visible at the start, and those due to more highly N_2-substituted species appear during photolysis. The band marked with an arrow in the final spectrum is seen to be the strongest absorption in this region and is due to tetrasubstituted molecule $Cr(CO)_2(N_2)_4$. The solution contains approximately 2.2 mmol of N_2 and 0.1 μmol of $Cr(CO)_6$. ($[N_2] \approx 0.25$ M, $[Cr(CO)_6] \approx 1.2 \times 10^{-5}$ M.) The pathlength of the cell was 2.7 cm.

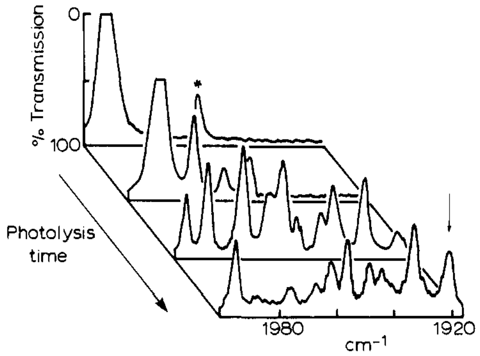

Figure 2. IR spectrum of a solution containing $Cr(CO)_6$ dissolved in a liquid Xe/N_2 mixture in the CO stretching region 2000–1915 cm^{-1}. The successive spectra have been recorded after progressively lengthier periods of photolysis. At the start the only IR absorptions are due to $Cr(CO)_6$. (The band marked with an asterisk is the natural-abundance carbon-13 satellite.) Absorptions due to more highly N_2-substituted species appear during photolysis. In the final spectrum the band marked with an arrow is due to $Cr(CO)_2(N_2)_4$.

Liquid-Xenon Experiments. The low-temperature/high-pressure cells, designed by Maier and Stewart, have been described previously.[9,15] They consist of a copper block with spectroscopic windows sealed with lead gaskets, cooled by pulses of liquid nitrogen. The length of these pulses is used to control the temperature, as monitored by a thermocouple calibrated by the freezing point of liquid Xe. The cells used here have volumes of 2.5 mL (1-cm pathlength) and 8.5 mL (2.7-cm pathlength) and can withstand pressures of ca. 225 psi, corresponding to the vapor pressure of liquid Xe at −35 °C. IR spectra were recorded with a Perkin-Elmer 283B spectrometer.

The final experiments in this series were performed with use of Nicolet MX-3600 FT IR spectrometer, which allowed the resolution (0.6 cm^{-1}) of closely spaced spectral features and also enabled more accurate frequency calibration than with the dispersive spectrometer.

UV/visible spectra were recorded with a prototype Perkin-Elmer Lambda 5 UV/vis spectrometer.

The experiments involved liquefying Xe/N_2 gas mixtures, doped with a measured amount of gaseous $Cr(CO)_6$, into the cooled cell and

---

(9) (a) Tyler, D. R.; Petrylak, D. P. *J. Organomet. Chem.* **1981**, *212*, 389–396. (b) Ozin, G. A.; Francis, C. G.; Huber, H. X.; Andrews, M.; Nazar, L. *J. Am. Chem. Soc.* **1981**, *103*, 2453.

(10) De Vore, T. C. *Inorg. Chem.* **1976**, *15*, 1315.

(11) Ford, T. A.; Huber, H.; Klotzbucher, W.; Ozin, G. A. *Inorg. Chem.* **1976**, *15*, 1666.

(12) Burdett, J. K.; Downs, A. J.; Gaskill, G. P.; Graham, M. A.; Turner, J. J.; Turner, R. F. *Inorg. Chem.* **1978**, *17*, 523.

(13) Graham, M. A. Ph.D. Thesis, Cambridge University, Cambridge, England, 1971.

(14) Timney, J. A. *Inorg. Chem.* **1979**, *18*, 2502.

(15) Beattie, W. H.; Maier II, W. B.; Holland, R. F.; Freund, S. M.; Stewart, B. *Proc. Soc. Photo-Opt. Instrum. Eng.* **1978**, *158*, 113.

Scheme I

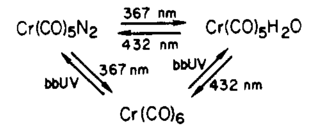

stirring the liquid magnetically to ensure that the $Cr(CO)_6$ was dissolved. After an IR spectrum had been recorded, the solution was briefly photolyzed, (Philips HPK-125W medium-pressure Hg arc), and another IR spectrum was recorded. IR spectra were then alternated with progressively longer and longer UV photolyses. For narrow-band photolysis at 367 and 432 nm Balzer interference filters (band-pass 20 nm) were employed.

III. Liquid-Xenon Experiments

Photochemistry in Liquid Xenon. Figures 1 and 2 show the IR spectra in the N–N and C–O stretching regions during successive stages in the UV photolysis of $Cr(CO)_6$ dissolved in a liquid Xe/N_2 mixture at −79 °C, as described in the Experimental Section. UV photolysis of $Cr(CO)_6$ in *pure* liquid Xe under these conditions rapidly destroyed the $Cr(CO)_6$, but no *new* IR bands were observed.

We have previously shown[8] that broad-band UV photolysis of $Cr(CO)_6$ in solution in liquid Xe containing a trace of N_2 generates $Cr(CO)_5N_2$. This photochemical process may be reversed by photolysis at 367 nm.

We have now measured the UV/vis spectra of liquid Xe solutions containing $Cr(CO)_5N_2$, and we see that this species has an absorption at λ_{max} = 365 nm. This value compares almost exactly with a previously reported[12] absorption maximum of this species in a solid matrix at 20 K.

Photolysis of $Cr(CO)_6$ at −79 °C, in solution in liquid Xe containing N_2 at a higher concentration, *initially* generates $Cr(CO)_5N_2$ (λ_{max} = 365 nm) and in some experiments another species, which is thermally stable at this temperature, with λ_{max} = 435 nm and IR absorptions at 1913.3, 1938.5/1944.2, 1975.5, and 2073.9 cm^{-1}. This species can be entirely destroyed by filtered photolysis at 432 nm. Moreover, it does not reappear on subsequent broad-band photolysis. We believe these data are consistent with this species being $Cr(CO)_5H_2O$ reported by Braterman et al.[16] (Scheme I). Particularly interesting is the splitting of the e mode expected for an $M(CO)_5L$ complex with an asymmetric ligand such as H_2O. Presumably the water arises from a trace impurity in the Xe or N_2 or, more probably, from incomplete degassing of the cell, since water is notoriously difficult to remove completely except in bakeable apparatus.

It should be emphasized that this species, $Cr(CO)_5H_2O$, appeared initially in *some* experiments during the earliest stages of photolysis in small quantities only, and there is no evidence that it plays any significant role in the subsequent photochemistry. So it is reasonable to suppose that all of the IR bands, in Figure 1 and 2, observed during prolonged photolysis in Xe/N_2 mixtures are due to $Cr(CO)_{6-x}(N_2)_x$ species. (N_2 was always present in substantial excess, i.e., $Cr(CO)_6$:N_2 = ca. 1:10^4—see Figure 1.) It is immediately clear that in both the N–N and C–O regions several IR bands appear to increase in intensity together and subsequently to decay; measurement of band intensity as a function of photolysis time confirms that some absorptions may be confidently linked together as a group, whereas other weaker bands may be only tentatively identified with a particular group (see Figure 3).

Additional evidence is available to assist in the assigning of bands together in groups. The species photolytically generated in solution are not all thermally stable at −79 °C or at higher temperatures. As the solution containing the product species is warmed, molecules of particular stoichiometries will become successively unstable and the IR absorptions of these thermally destabilized molecules will disappear as the species decays. Figure 4 shows a series of successive spectra taken at −79 °C, from which it is clear that the bands marked with an arrow (↑) decay together. Equally importantly, the final spectrum clearly shows that the band marked with an asterisk (*) incorporates another absorption from a species that is more stable at −79 °C. Similar experiments were performed in the temperature region −55 to −50 °C.

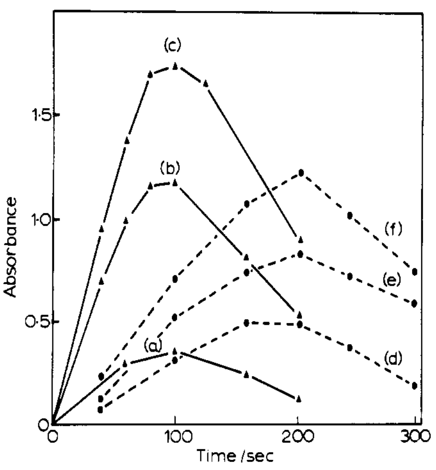

Figure 3. Dependence of band intensity on total photolysis time for two groups of bands, for the photolysis of $Cr(CO)_6$ dissolved in a liquid Xe/N_2 mixture: (—) band group II, (a) = 2051.9 cm^{-1}, (b) = 1943.2 cm^{-1}, (c) = 1961.3 cm^{-1}; (---) band group III, (d) = 1947.2 cm^{-1}, (e) = 1994.6 cm^{-1}, (f) = 1931.8 cm^{-1}. Note how the maximum intensity of band group II occurs much earlier than that of group III, indicating a lower degree of N_2 substitution.

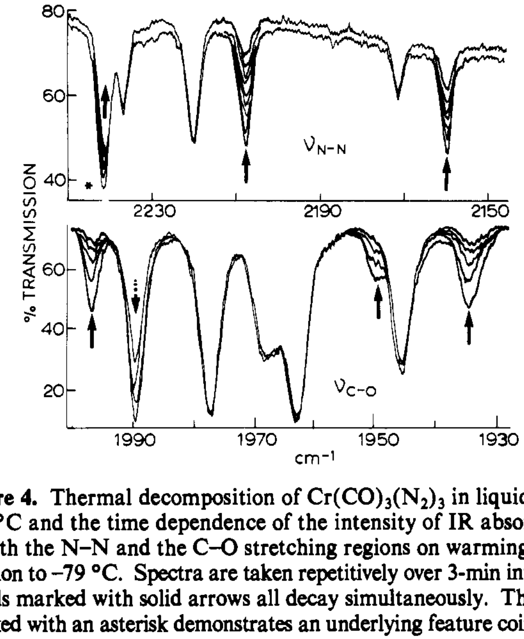

Figure 4. Thermal decomposition of $Cr(CO)_3(N_2)_3$ in liquid Xe at −79 °C and the time dependence of the intensity of IR absorptions in both the N–N and the C–O stretching regions on warming of the solution to −79 °C. Spectra are taken repetitively over 3-min intervals. Bands marked with solid arrows all decay simultaneously. The band marked with an asterisk demonstrates an underlying feature coincident with the decaying absorption. The band marked with a dashed arrow is due to $Cr(CO)_6$, and it *increases* in intensity, probably due to undissolved $Cr(CO)_6$ dissolving slowly at the higher temperature.

An initial interpretation of these data may be made on the basis of two assumptions.

(i) Progressive broad-band UV photolysis will tend to generate coordinatively saturated species $Cr(CO)_{6-x}(N_2)_x$ with increasing values of x.

(ii) We would expect that, as the value of x in $Cr(CO)_{6-x}(N_2)_x$ increases, the species will become less stable. So the lower the temperature at which thermal decay begins

---

[16] Boylan, M. J.; Black, J. D.; Braterman, P. S. *J. Chem. Soc., Dalton Trans.* **1980**, 1646.

for a particular species, the more highly N_2 substituted that species is.

These two assumptions may be applied to both methods of linking the IR absorptions together in band groups, to produce an interim assignment. The result of this process is shown in Table I and Chart I.

Table I. Wavenumbers and Relative Intensities of IR Bands of $Cr(CO)_{6-x}(N_2)_x$ Species[c]

band group	wavenumber,[a] cm^{-1}	approx rel intens[b]	band group	wavenumber,[a] cm^{-1}	approx rel intens[b]
0	2010.0	...	III	(2241.3)	(0.4)
	1987.1	...		(2207.2)	(1)
	1958.7			(2186.3)	(0.1)
I	(2236.6)	...		2159.3	1
	2086.4	0.05		2023.0	vw
	1974.9	1		1994.6	0.7
	1964.9	0.3		1947.2	0.3
II	(2240.8)	(1)		1939.6	1
	(2219.8)	(1)		1931.8	
	(2170.6)	(0.5)	IV	(2233.5)	(w)
	2051.9	0.1		(2193.5)	(0.3)
	1966.8	1		(2165.0)	(vw)
	1961.3	0.5		(2142.4)	(1)
	1943.2			1919.6	1
			V	(2122.5)	...

[a] Entries in parentheses refer to absorptions assigned subsequently to N-N stretching vibrations. Other bands are assigned to C-O stretchings. [b] The intensity values refer to relative peak heights of CO or NN vibrations within a particular band group. There is no quantitative implication of the relative intensities of CO and NN vibrations. Generally, the CO absorptions are much more intense than the NN bands. [c] The bands are grouped on the basis of photochemical and thermal behavior.

Chart I. The Series $Cr(CO)_{6-x}(N_2)_x$

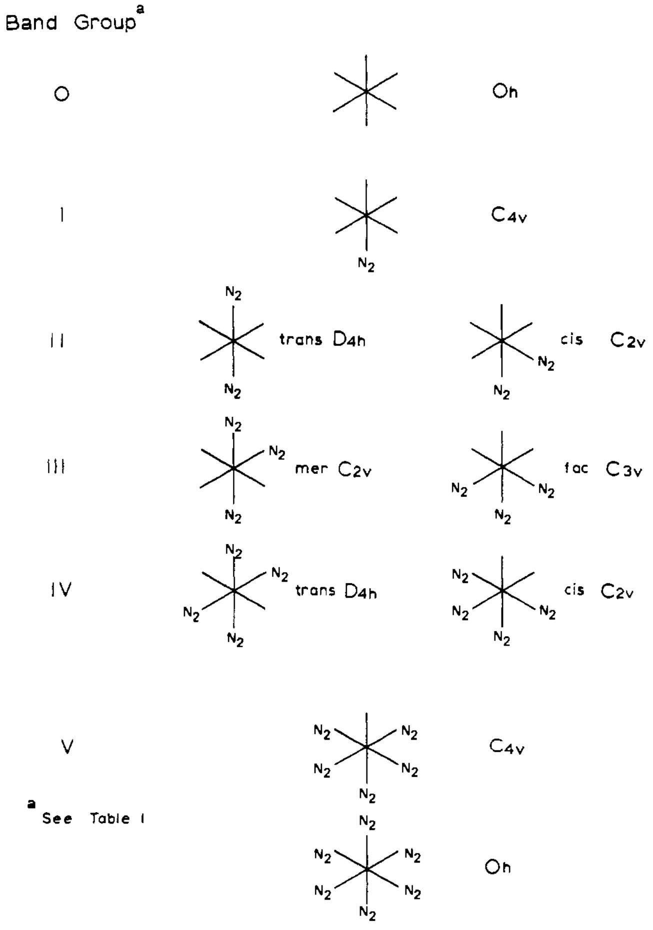

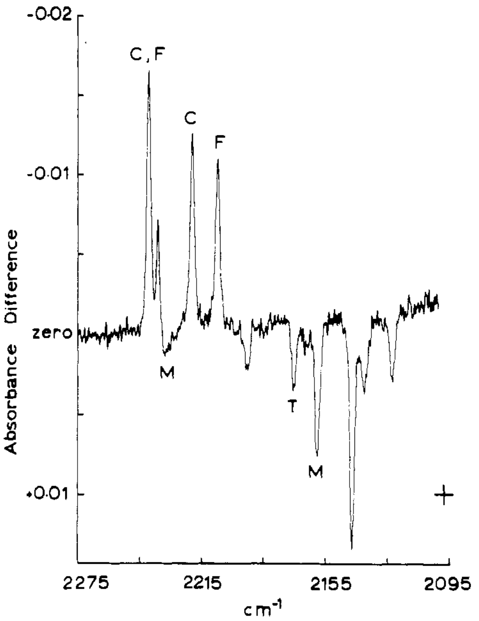

Figure 5. FT IR difference spectrum in the $\bar{\nu}_{NN}$ region, obtained by computer subtraction (spectrum recorded after 367-nm photolysis *minus* spectrum before photolysis) of a liquid-Xe solution of $Cr(CO)_{6-x}(N_2)_x$ species. Negative peaks indicate species that *decrease* upon photolysis; conversely, positive peaks indicate species that *increase* on photolysis. The peaks are labeled C for *cis*-$Cr(CO)_4(N_2)_2$, T for *trans*-$Cr(CO)_4(N_2)_2$, F for *fac*-$Cr(CO)_3(N_2)_3$, and M for *mer*-$Cr(CO)_3(N_2)_3$. Note that photolysis at this wavelength distinguishes between the pairs of isomers cis/trans and *mer*/*fac*.

Once the IR absorptions have been grouped together (on the basis of their respective thermal and photochemical behavior) according to the number of N_2 groups in the molecules to which they belong, additional evidence is available to distinguish between different isomers, e.g., *cis*- and *trans*-$Cr(CO)_4(N_2)_2$ or *fac*- and *mer*-$Cr(CO)_3(N_2)_3$.

Narrow-band photolysis at 367 nm of a liquid Xe solution containing $Cr(CO)_6$ and a wide range of N_2-substituted species, $Cr(CO)_{6-x}(N_2)_x$, destroys some species and leaves others relatively unaffected. Moreover, at this wavelength (corresponding to d–d transitions) different geometric isomers will be expected to have significantly different absorption cross sections, so we may expect to see in a subtraction spectrum, e.g., Figure 5 (before 367 nm–after 367 nm), some absorptions increasing and others decreasing.

Some of the assignments implied by Chart I and Table I anticipate the conclusions of later sections of this paper. The remainder of the paper sets out in detail our reasons for proposing these assignments.

Intensities of C–O and N–N Stretching Vibrations. Carbonyl band intensities have been of very considerable help both in assigning spectra and in determining structures.[17] The simple local oscillating dipole method seems to work well,[17,18] provided there are no other ligands that can couple with the carbonyl modes. Clearly with N_2 as a ligand, there is substantial coupling, so we can only expect such assignments to be qualitative. However, any assignment of bands must not be in gross contradiction of predicted intensities. Furthermore, we can surely suppose that, in spite of the dearth of information on intensities of N–N stretching bands, the pattern of band intensities will mimic the C–O behavior. Certainly Ozin's work on $Ni(N_2)_x$ ($x = 1$–4) suggests that this is so.[4]

---

(17) (a) Darling, J. H.; Ogden, J. S. *J. Chem. Soc., Dalton Trans.* **1972**, 2496. (b) Haines, L. M.; Stiddard, M. B. H. *Adv. Inorg. Chem. Radiochem.* **1970**, *12*, 53.

(18) Burdett, J. K.; Poliakoff, M.; Turner, J. J. *Adv. Infrared Raman Spectrosc.* **1976**, *2*, 1.

Table II. Predicted Relative Intensities for $\bar{\nu}_{NN}$ and $\bar{\nu}_{CO}$ Bands of $Cr(CO)_{6-x}(N_2)_x$

species	sym	rel IR band intens[a] $\bar{\nu}_{CO}$[b]		$\bar{\nu}_{NN}$[b]	
$Cr(CO)_6$	O_h	t_{1u}	6	...	...
$Cr(CO)_5N_2$	C_{4v}	a_1	} 1	a_1	1
		a_1			
		e	4		
trans-$Cr(CO)_4(N_2)_2$	D_{4h}	e_u	4	a_{2u}	2
cis-$Cr(CO)_4(N_2)_2$	C_{2v}	a_1	} 1	a_1	1
		a_1		b_2	1
		b_1	2		
		b_2	1		
fac-$Cr(CO)_3(N_2)_3$	C_{3v}	a_1	1	a_1	1
		e	2	e	2
mer-$Cr(CO)_3(N_2)_3$	C_{2v}	a_1	} 1	a_1	} 1
		a_1		a_1	
		b_2	2	b_1	2
trans-$Cr(CO)_2(N_2)_4$	D_{4h}	a_{2u}	2	e_u	4
cis-$Cr(CO)_2(N_2)_4$	C_{2v}	a_1	1	a_1	} 1
		b_1	1	a_1	
				b_1	2
				b_2	1
$Cr(CO)(N_2)_5$	C_{4v}	a_1	1	a_1	} 1
				a_1	
				e	4
$Cr(N_2)_6$	O_h	...	...	t_{1u}	6

[a] Intensity values are predicted on the basis of a simple local oscillating dipole model;[19] see text. [b] Note that the values given refer to the relative intensities of *either* CO *or* NN vibrations for a particular molecule. The CO and NN intensities are independent of each other.

Using the simplest possible approach, which was originally described by Orgel,[19] we can predict the approximate intensities for the various modes of all possible $Cr(CO)_{6-x}(N_2)_x$ species (Table II).

Approximate Force Fields and C–O Stretching Vibrations. For the purpose of the assignment of vibrational bands of metal carbonyls, the energy-factored force field is entirely adequate.[20] Moreover, it works well for N–N bands of dinitrogen complexes, as shown by matrix studies on $M(N_2)_x$ complexes.[4] However, because of the vibrational coupling between N_2 and CO groups, is it valid to treat the CO groups in $Cr(CO)_{6-x}(N_2)_x$ as an isolated $Cr(CO)_{6-x}$ fragment and the NN groups as an isolated $Cr(N_2)_x$ fragment? Examination of the spectra of $Ni(CO)_x(N_2)_y$, $Mo(CO)_5N_2$, and other species suggest that this separation is a reasonable approximation, with energy-factored CO (and NN) force constants perturbed by coupling with N_2 (and CO) groups. However, it has been shown[21] that, where such CO–NN coupling exists, simple intensity rules are even less reliable than usual.

The problem in the present case is to "guess" the values of the force constants in order to predict sets of frequencies to correlate with those observed in the photochemical solution experiments. Fortunately, Timney[14] has developed a simple, but extremely powerful, empirical method for predicting energy-factored C–O force constants. Briefly, with concentration on a relevant system such as $Cr(CO)_{6-x}L_x$

$$k_{CO} = k_d + \sum_{CO} \epsilon_{CO}{}^{\theta} + \sum_{L} \epsilon_{L}{}^{\theta} \qquad (1)$$

where k_d is the force constant for the isolated metal monocarbonyl fragment CrCO (e.g., from matrix studies) and $\epsilon_L{}^{\theta}$ and $\epsilon_{CO}{}^{\theta}$ are the "ligand-effect constants", which, for a particular ligand L or CO, quantify the effect on k_d of adding L or CO to CrCO at an angle θ. The assumption, verified by Timney, is that the effects are additive. Thus, for *mer*-$Cr(CO)_3(N_2)_3$ (**1**), $k_1 = k_d + \epsilon_{CO}{}^{90} + \epsilon_{CO}{}^{180} + 3\epsilon_{N_2}{}^{90}$ and $k_2 = k_d + 2\epsilon_{CO}{}^{90} + \epsilon_{N_2}{}^{180} + 2\epsilon_{N_2}{}^{90}$. The values of the appropriate ϵ values are given in Table IIIA. In view of the limited number of N_2-substituted carbonyls used by Timney to derive ϵ_{N_2}, these values are likely to be inaccurate, particularly at high levels of N_2 substitution.

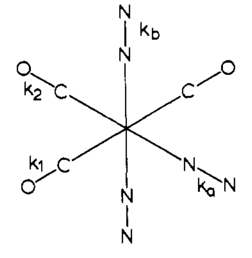

1

It is necessary to know the interaction as well as the principal force constants to predict the C–O stretching spectrum, and Timney showed that these interaction constants could be reliably estimated from eq 2, where A and B depend only on the

$$k_{12} = A - B\left(\frac{k_1 + k_2}{2}\right) \qquad (2)$$

angle between the two CO groups involved. The values for 90 and 180° are shown in Table IIIA.

Thus, it is possible, on the basis of Timney's semiempirical argument, to predict the freuencies of all the carbonyl stretching modes of all the species $Cr(CO)_{6-x}(N_2)_x$. Similar calculations can be made for the N–N vibrations.[22]

Given the simplicity of Timney's method, it is worth asking whether some marginal alteration of the parameters might not be effective in improving the fit between observed and calculated frequencies. Several minor modifications were tried, but the simplest and most effective was to ignore the small variations in interaction force constant implied by the expression for k_{12} (eq 2) and to fix $k_{12}{}^{cis}$ and $k_{12}{}^{trans}$ at 30 and 52 N m^{-1}, respectively, and to use new values of $\epsilon_{N_2}{}^{90}$ (13.0 N m^{-1}) and $\epsilon_{N_2}{}^{180}$ (59.5 N m^{-1}). Table IIIB summarizes the result of calculations with these parameters, compared with the experimental data from Table I.

There is reasonable agreement between prediction and observation for the ν_{CO} modes in terms of both frequency and relative intensity (see section IV for a detailed discussion of relative intensities).

It is perhaps surprising that the b_2 mode of *mer*-$Cr(CO)_3(N_2)_3$ is so much weaker than expected in comparison with the e mode of the *fac* isomer, suggesting perhaps that the *mer* isomer is present in less than statistical amounts. The absence of other bands can be understood in terms of overlap. For example, the missing a_{2u} band of *trans*-$Cr(CO)_2(N_2)_4$ should lie close to the strong e band of *fac*-$Cr(CO)_3(N_2)_3$. Thus, overall consistency with the framework of assignments proposed is demonstrated.

With some limitations, Timney's method may be extended to the N–N stretching vibrations of the mixed species, $Cr(CO)_{6-x}(N_2)_x$. For a molecule such as **1** we need to know k_a, k_b, and the cis and trans interaction force constants before predicting the N–N frequencies. There is no large body of data available for mixed carbonyl–dinitrogen species from

---

[19] Orgel, L. E. *Inorg. Chem.* **1962**, *1*, 25.

[20] (a) Kraihanzel, C. S.; Cotton, F. A. *J. Am. Chem. Soc.* **1962**, *84*, 4432. (b) Cotton, F. A. *Inorg. Chem.* **1964**, *3*, 702. (c) Haas, H.; Sheline, R. K. *J. Chem. Phys.* **1967**, *47*, 2996.

[21] Burdett, J. K. *Inorg. Chem.* **1981**, *20*, 2607.

[22] Many of these calculations were carried out by R. Howsely as part of his undergraduate project, Fall 1980.

[23] This brief photolysis removes any $Cr(N_2)_6$ or $Cr(N_2)_4$[10] that may have been formed during deposition.

Table III

A. Parameters Used in Approximate Force Field Calculations[14]

Angle (θ), deg	ligand-effect const, N m^{-1}		"interaction" parameters,[b] N m^{-1}	
	$\epsilon_{CO}{}^{\theta}$	$\epsilon_{N_2}{}^{\theta}$	*A*	*B*
90	33.5	14.0 (13.0)[a]	180	0.0929
180	126.1	52.0 (59.5)[a]	241	0.113

B. Observed and Predicted Wavenumbers of $\bar{\nu}_{CO}$ and $\bar{\nu}_{NN}$ IR Bands of $Cr(CO)_{6-x}(N_2)_x$ Species

band group[c]	$\bar{\nu}_{NN}$				species	$\bar{\nu}_{CO}$			
	wavenumber, cm^{-1}						wavenumber, cm^{-1}		
	obsd[a]	pred[e,g]	$\Delta\nu$[f]	mode		mode	obsd[d]	pred[e]	$\Delta\nu$[f]
0					$Cr(CO)_6$ (O_h)	t_{1u}	2010.0		
							1987.1	1987.5	−0.4
							1958.7		
I	2236.6	2236.4	0.2	a_1	$Cr(CO)_5N_2$ (C_{4v})	a_1	2086.4	2086.9	−0.5
						a_1	1964.9	1965.7	−0.8
						e	1974.9	1974.6	0.3
II	2240.8	2237.2	3.6	a_1	*cis*-$Cr(CO)_4(N_2)_2$ (C_{2v})	a_1	2051.9	2047.6	4.3
	2219.8	2213.2	6.6	b_2		a_1	1966.8	1962.4	4.2
						b_1	1961.3	1961.7	−0.4
						b_2	1943.2	1946.5	−3.3
	2170.6	2170.9	−0.3	a_{2u}	*trans*-$Cr(CO)_4(N_2)_2$ (D_{4h})	e_u	1961.3	1961.7	−0.4
III	2241.3	2238.0	3.3	a_1	*fac*-$Cr(CO)_3(N_2)_3$ (C_{3v})	a_1	1994.6	1990.2	4.4
	2207.2	2202.0	5.2	e		e	1931.8	1933.4	−1.6
	2233.5	2232.8	0.7	a_1	*mer*-$Cr(CO)_3(N_2)_3$ (C_{2v})	a_1	2023.0	2023.4	−0.4
	2186.3	2198.6	−12.3	a_1		a_1	1939.6	1942.5	−2.9
	2159.3	2159.4	−0.1	b_1		b_2	1947.2	1948.8	−1.6
IV	2233.5	2234.9	−1.4	a_1	*cis*-$Cr(CO)_2(N_2)_4$ (C_{2v})	a_1	1955.4	1958.5	−3.1
	2165.0	2185.9	−20.9	a_1		b_1	1919.6	1920.2	−0.6
	2142.4	2147.8	−5.4	b_1					
	2193.5	2190.6	2.9	b_2					
	2142.4	2147.8	−5.4	e_u	*trans*-$Cr(CO)_2(N_2)_4$ (D_{4h})	a_{2u}	. . .	1935.7	. . .
V	. . .	2233.1	. . .	a_1	$Cr(CO)(N_2)_5$ (C_{4v})	a_1	. . .	1926.3	. . .
	. . .	2177.3	. . .	a_1					
	2122.5	2136.2	−13.7	e					
	h	2124	. . .	t_{1u}	$Cr(N_2)_6$ (O_h)				

[a] Revised values (see text). [b] See eq 2. [c] Bands grouped as in Table I. [d] Observed values for liquid-Xe solutions, −79 °C. [e] Predicted with Timney's method,[14] with use of the parameters in Table IIIA. [f] Observed minus predicted wavenumber. [g] With revised parameters (see Table IIIA and text). [h] See text for band assigned to this molecule in matrix cocondensation experiments.

which to estimate reliably the necessary parameters, so rather more drastic assumptions become necessary. When Timney's basic hypothesis of additive ligand-effect constants, ϵ, is recalled

$$k_a = k_d' + 2\epsilon'_{N_2}{}^{90} + \epsilon'_{N_2}{}^{180} + 2\epsilon'_{CO}{}^{90} \qquad (3)$$

The simplest possible assumption is that $\epsilon' \equiv \epsilon$; i.e., the ligand effect constants for $\bar{\nu}_{NN}$ and $\bar{\nu}_{CO}$ are identical. Given[8] that, for $Cr(CO)_5N_2$, $\bar{\nu}_{NN}$ is 2236.5 cm^{-1}, it is possible to calculate that k_d', the frequency-factored N–N force constant for an isolated Cr–N_2 group, has the value 1803 N m^{-1}. Thus, it is possible to estimate any energy-factored principal N–N force constant.

For the interaction force constants the simplest assumption is that they are close to the C–O interaction force constants. Some support for this seemingly rash assertion may be cited in that, for $Ni(CO)_4$, $k_{CO,CO}$[14] is 34 N m^{-1} and, for $Ni(N_2)_4$, k_{N_2,N_2}[4] is 32 N m^{-1}. With these simplifying assumptions $\bar{\nu}_{NN}$ for the series $Cr(CO)_{6-x}(N_2)_x$ may be calculated as shown in Table IIIB. The ligand-effect constants ($\epsilon'_{N_2}{}^{\theta}$) and interaction force constants used in the calculation are shown in Table IIIA. The ligand-effect constants are identical in value with those used for the $\bar{\nu}_{CO}$ calculation, but the interaction force constants have been varied slightly to provide the best fit. Given the obvious crudity of the model, the agreement is striking and lends confidence to the assignments. No doubt further adjustments to the force constants would improve the fit, but it hardly seems profitable.

Clearly the use of variable parameters weakens the predictive power of Timney's method, in an area where there are few experimental data for comparison. The purpose of this section has not been to demonstrate a priori absolute assignments of the observed bands but rather to show consistency with a general model that allows us to proceed with some confidence in assigning the bands on the basis of direct experimental information.

IV. Detailed Assignments of $Cr(CO)_{6-x}(N_2)_x$ Species in Liquid Xenon

We have outlined, in the previous three sections, our experimental observations consisting of the IR spectroscopic examination of species produced by the broad-band UV photolysis of $Cr(CO)_6$ dissolved in a liquefied Xe/N_2 mixture, the arrangement of those absorptions into groups of IR bands, and the way in which assignment of these band groups may be confirmed on the basis of comparison with theoretical predictions of band frequencies and intensities for the series $Cr(CO)_{6-x}(N_2)_x$. It is appropriate to gather together the conclusions of this analysis.

Band Group 0—$Cr(CO)_6$. The assignment of bands in this group is somewhat trivial. The band at 1987.1 cm^{-1} is the t_{1u} mode of $Cr(CO)_6$ in liquid Xe; the 1958.7-cm^{-1} absorption is the most intense observable band of $Cr(^{12}CO)_5(^{13}CO)$ present in (6.4%) natural abundance—of the other three bands of this species, one lies under the t_{1u} band of $Cr(CO)_6$, one is observed at 2010.0 cm^{-1}, and one is predicted to be at higher frequency and considerably less intense.

Band Group I—$Cr(CO)_5N_2$. In published work[8,12] the bands in this group have been unambiguously assigned to $Cr(CO)_5N_2$. The confidence in this assignment derives from a

Table IV. Wavenumbers and Intensities of Group II–IV Bands with Assignments

A. Group II

cis-$Cr(CO)_4(N_2)_2$			*trans*-$Cr(CO)_4(N_2)_2$		
wavenumber, cm^{-1}	mode	intens[a]	wavenumber, cm^{-1}	mode	intens[a]
2240.8	$a_1\ \bar{\nu}_{NN}$	1	2170.6	$a_{2u}\ \bar{\nu}_{NN}$	0.5
2219.8	$b_2\ \bar{\nu}_{NN}$	1			
2051.9	$a_1\ \bar{\nu}_{CO}$	0.2			
1966.8	$a_1\ \bar{\nu}_{CO}$	0.5			
1961.3	$b_1\ \bar{\nu}_{CO}$	2	1961.3	$e_u\ \bar{\nu}_{CO}$	?
1943.2	$b_2\ \bar{\nu}_{CO}$	1			

B. Group III

fac-$Cr(CO)_3(N_2)_3$			*mer*-$Cr(CO)_3(N_2)_3$		
wavenumber, cm^{-1}	mode	intens[a]	wavenumber, cm^{-1}	mode	intens[a]
2241.3[b]	$a_1\ \bar{\nu}_{NN}$	0.4	2233.5	$a_1\ \bar{\nu}_{NN}$	w
2207.2	$e\ \bar{\nu}_{NN}$	1	2186.3	$a_1\ \bar{\nu}_{NN}$	0.1
1994.6	$a_1\ \bar{\nu}_{CO}$	0.7	2159.3	$b_1\ \bar{\nu}_{NN}$	1
1931.8	$e\ \bar{\nu}_{CO}$	1	2023.0	$a_1\ \bar{\nu}_{CO}$	vw
			1947.2	$b_2\ \bar{\nu}_{CO}$	0.3
			1939.6	$a_1\ \bar{\nu}_{CO}$	0.1

C. Group IV

cis-$Cr(CO)_2(N_2)_4$			*trans*-$Cr(CO)_2(N_2)_4$		
wavenumber, cm^{-1}	mode	intens[a]	wavenumber, cm^{-1}	mode	intens[a]
2233.5[c]	$a_1\ \bar{\nu}_{NN}$	w	2142.4	$e_u\ \bar{\nu}_{NN}$	. . .
2165.0	$a_1\ \bar{\nu}_{NN}$	vw			
2142.4	$b_1\ \bar{\nu}_{NN}$	1	*d*	$a_{2u}\ \bar{\nu}_{CO}$	
2193.5	$b_2\ \bar{\nu}_{NN}$	0.3			
1955.4	$a_1\ \bar{\nu}_{CO}$	1			
1919.6	$b_1\ \bar{\nu}_{CO}$	1			

[a] The intensity values refer to relative intensities of $\bar{\nu}_{CO}$ *or* $\bar{\nu}_{NN}$ bands. No indication of the relative intensity of $\bar{\nu}_{CO}$ *and* $\bar{\nu}_{NN}$ absorptions is implied. [b] High-resolution FT IR data separate this band from the nearly coincident absorption due to *cis*-$Cr(CO)_4(N_2)_2$. [c] Uncertain assignment. See group III bands above. [d] Not observed.

comparison of the solution data with those of the species trapped in solid matrices examined by IR and Raman spectroscopy and completely characterized by isotopic substitution. For completeness, the solution and matrix data are reproduced in Table V. The relative intensities of the $\bar{\nu}_{CO}$ a_1 and e modes in liquid-Xe solution are very similar to those observed in matrices and to those expected on simple theoretical grounds (Table II).

Band Group II—$Cr(CO)_4(N_2)_2$. The bands of this group are best assigned as in Table IVA.

The distinction between cis and trans isomers is readily made on the basis of narrow-band photolysis at 367 nm (see Figure 5). The fact that the cis isomer is relatively more affected by this photolysis can be easily rationalized.

All d → d transitions are forbidden in the trans isomer, which is centrosymmetric. Thus, the absorption cross section at 367 nm of the cis isomer, C_{2v}, would be expected to be higher than that of the trans, D_{4h}, and so, on photolysis at this wavelength, the cis isomer will absorb light preferentially. The growth in bands assigned to higher substituted N_2 complexes, e.g., $Cr(CO)_2(N_2)_4$, during 367-nm irradiation suggests that the isomerization is due to dissociation followed by recombination with N_2 rather than an intramolecular process.

The expected ratio of the intensities of the $\bar{\nu}_{CO}$ bands of the cis isomer is $b_2{:}b_1{:}a_1 + a_1 = 1{:}2{:}1$ (Table II); for the $\bar{\nu}_{NN}$ bands the expected ratio is $a_1{:}b_2 = 1{:}1$. The observed relative intensities are in rough agreement. Note that the $\bar{\nu}_{CO}$ absorption at 1961.3 cm^{-1} is assigned to both the cis and the trans isomers, consistent with the application of a frequency-factored force field. Consequently, it is not possible to determine the relative abundance of cis and trans isomers from this band alone. However, in this case the $\bar{\nu}_{NN}$ band of the trans isomer does appear at 2170.6 cm^{-1}, indicating that some of the intensity at 1961.3 cm^{-1} is due to this species. The expected statistical probability of cis:trans isomers is 4:1.

Band Group III—$Cr(CO)_3(N_2)_3$. The bands in this group are best assigned as in Table IVB. Again the distinction between isomers is confirmed by 367-nm photolysis.

The assignment for the *fac* isomer is relatively straightforward. The a_1 $\bar{\nu}_{NN}$ band at 2241.3 cm^{-1} is nearly identical in frequency with the a_1 $\bar{\nu}_{NN}$ absorption of the *cis*-$Cr(CO)_4(N_2)_2$ species, but this band overlap was clearly detected as a consequence of the two molecules' different thermal stabilities and is demonstrated in Figure 4. The intensity ratios of a_1:e modes are in reasonable agreement with those expected (Table II).

For the *mer*-$Cr(CO)_3(N_2)_3$ isomer the position is less obvious. The bands are generally lower in intensity despite a predicted statistical distribution which would suggest a ratio *mer:fac* of 3:2. It is, of course, entirely possible that thermodynamic or kinetic factors should intervene and perturb the geometrical distribution of products in the photolysis. The weak band at 2233.5 cm^{-1} is assigned tentatively as a_1 $\bar{\nu}_{NN}$, although it is not really possible on grounds of intensity, force field, or photochemical behavior to link it unambiguously with *mer*-$Cr(CO)_3(N_2)_3$—it could just as properly be assigned as the a_1 $\bar{\nu}_{NN}$ for *cis*-$Cr(CO)_2(N_2)_4$ (see below).

Band Group IV—$Cr(CO)_2(N_2)_4$. The bands in this group can be reasonably assigned as in Table IVC. There is no gross contradiction between observed and expected relative intensities. In this case, however, the a_{2u} mode of the trans isomer is not observed, so there is no indication how much, if any, of this species is present since the $\bar{\nu}_{NN}$ mode is degenerate with the corresponding cis isomer. The expected position of the a_{2u} mode is close to that of an intense *fac*-$Cr(CO)_3(N_2)_3$ band.

Band Group V—$Cr(CO)(N_2)_5$. This weak band at 2122.5 cm^{-1} is best assigned to the e $\bar{\nu}_{NN}$ mode of $Cr(CO)(N_2)_5$. In some spectra another weak feature similar in intensity to that of the 2122.5-cm^{-1} band is observed at 2136.2 cm^{-1}. No absorption in the carbonyl region can be linked with either band. On the evidence available it is not really possible to assign either absorption unambiguously to $Cr(CO)(N_2)_5$ or $Cr(N_2)_6$. Obviously it is possible that the 2136.2-cm^{-1} band is the e $\bar{\nu}_{NN}$ mode of $Cr(CO)(N_2)_5$ and the 2122.5-cm^{-1} band is the t_{1u} $\bar{\nu}_{NN}$ for $Cr(N_2)_6$. However, in the matrix, $Cr(N_2)_6$ absorbs at 2112 cm^{-1} and $Cr(CO)(N_2)_5$ at 2127 cm^{-1} (see below). For the other species such as $Cr(CO)_2(N_2)_4$ $\bar{\nu}_{NN}$(matrix) − ν_{NN}(Xe solution) is about 4–8 cm^{-1} so the likelihood is that the 2122.5-cm^{-1} absorption in liquid Xe should be assigned to e $\bar{\nu}_{NN}$ of $Cr(CO)(N_2)_5$. It was not possible to generate in solution a sufficiently high concentration of this highly unstable species to observe the $\bar{\nu}_{CO}$ band. This difficulty can be overcome by comparing our results with those of matrix isolation experiments.

V. Matrix Isolation Experiments

We have previously[12,13,24] conducted matrix isolation experiments on the $Cr/CO/N_2$ system (both by photolysis of $Cr(CO)_6/N_2$ mixtures and by cocondensation of Cr atom/CO/N_2 mixtures) in an attempt to generate the species $Cr(CO)_{6-x}(N_2)_x$. The results proved essentially uninterpretable for the reasons outlined in the Introduction, which are general for the application of the matrix isolation technique to complex systems. In the light of the data for liquid-Xe solution (see above) we can now reexamine the matrix data for corre-

---

(24) Turner, R. F. Ph.D. Thesis, University of Newcastle-upon-Tyne, Newcastle-upon-Tyne, England, 1976.

Table V. Wavenumbers (cm^{-1}) of IR Bands of $Cr(CO)_5N_2$ in Liquid-Xe Solution and Ar Matrix

liquid Xe (194 K)	Ar matrix[a] (10 K)	assignt	liquid Xe (194 K)	Ar matrix[a] (10 K)	assignt
2236.6	2243	(NN) a_1	1974.9	1975	(CO) e
2086.4	2088	(CO) a_1	1964.9	1962	(CO) a_1

[a] Taken from ref 12.

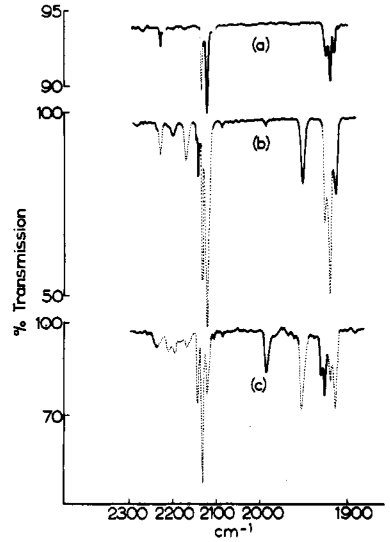

Figure 6. IR spectra of matrices prepared by the cocondensation of Cr atoms with N_2/CO mixtures: (a) N_2 containing a trace of CO + 10 min of photolysis[23] with 280 > λ > 390 nm (bands due to $Cr(CO)(N_2)_5$ are marked with a solid line); (b) 100:1 mixture of N_2 and $C^{16}O$, + 10 min of photolysis at λ > 375 nm (additional bands due to $Cr(CO)_2(N_2)_4$ are marked with a solid line); (c) 100:1 mixture of N_2 and $C^{16}O$ + 40 min of photolysis with an unfiltered mercury lamp (additional bands due to *fac*-$Cr(CO)_3(N_2)_3$ are marked with a solid line). All spectra were recorded at 20 K and taken from ref 13 but reassigned as explained in the text.

spondences with the results described and also check for any anomalies between matrix and solution experiments. If the assignments are correct, we expect close correspondence, on the basis of the $Cr(CO)_5N_2$ comparison (see Table V). In particular, the matrix experiments provide information about the $Cr(CO)_2(N_2)_4$ and $Cr(CO)(N_2)_5$ species, where the solution data were rather sparse, and support these assignments with $C^{18}O$ enrichment, which was too complicated for the solution experiments.

Cocondensation Experiments. In these experiments Cr atoms were cocondensed with mixtures of N_2 and CO onto a CsBr window at 20 K, forming $Cr(CO)_{6-x}(N_2)_x$ species. It is clear that x will increase as the ratio N_2:CO is increased, and so by varying this ratio we can crudely choose which species to synthesize. Thus, after cocondensation of Cr + N_2:CO (200:1), bands due to $Cr(CO)(N_2)_5$ predominate (see Figure 6a; the assignment of these bands is discussed below), while at 100:1 the bands of $Cr(CO)_2(N_2)_4$ are clearly visible (Figure 6b).

It is not immediately obvious that subsequent UV or visible photolysis of such a cocondensed matrix will decrease the value of x (i.e., will produce complexes containing more CO). Nevertheless, comparison of the spectra in Figure 6b,c will show this is so, since photolysis reduces the intensity of the bands of $Cr(CO)(N_2)_5$ and increases those of $Cr(CO)_3(N_2)_3$. Although these experiments provide a crude assignment of the bands to various $Cr(CO)_{6-x}(N_2)_x$ species, we need other data for a more precise interpretation. Also, in general, the cocondensation experiments have only provided reliable data in $\bar{\nu}_{CO}$ region.

Table VI

A. Comparison between Data from Matrix Cocondensation and Liquid-Xe Solution Photochemistry Experiments for $Cr(CO)(N_2)_5$

band	$\bar{\nu}$(soln),[a] cm^{-1}	$\bar{\nu}$(matrix),[b] cm^{-1}	I_{obsd}[d]	approx force field,[c] cm^{-1}	I_{pred}[d]
a_1 (NN)	...	2236	0.4	2233	} 1
a_1 (NN)	...	...	...	2177	
e (NN)	2122.5	2127	4	2136	4
a_1 (CO)	...	1927[e] 1921	...	1926	...

B. Wavenumbers of $\bar{\nu}_{CO}$ in an N_2 Matrix Doped with a 1:1 Mixture of $C^{16}O/C^{18}O$ for $Cr(CO)(N_2)_5$

$\bar{\nu}(C^{16}O)$,[f] cm^{-1}	$\bar{\nu}(C^{18}O)$,[g] cm^{-1}	$\bar{\nu}(C^{16}O)$,[f] cm^{-1}	$\bar{\nu}(C^{18}O)$,[g] cm^{-1}
1927	1884	1921	1878.1

[a] Data from liquid-Xe solution photochemistry (Table IV).
[b] Data from the matrix cocondensation experiment (Figure 6).
[c] Predicted values from the Timney method (Table IIIB).
[d] Approximate relative intensities, observed and predicted.
[e] Matrix-split group of bands; see Table VIB. [f] Matrix-split group of bands; see Table VIA. [g] See Figure 7 for spectrum and details of conditions.

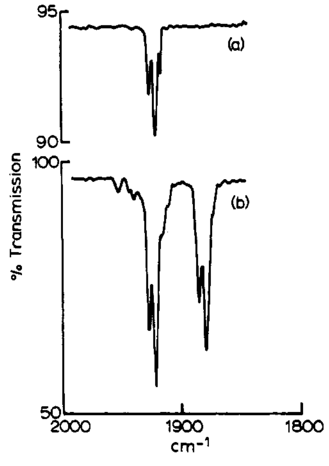

Figure 7. IR spectra for $Cr(CO)(N_2)_5$ in the $\bar{\nu}_{CO}$ frequency range: (a) matrix obtained with the same mixture as in Figure 6a; (b) matrix obtained by the cocondensation of Cr atoms with a 200:1:1 mixture of N_2, $C^{16}O$, and $C^{18}O$.

$Cr(CO)(N_2)_5$. In Figure 6a, the band at 2127 cm^{-1} compares well with the band at 2122.5 cm^{-1} from the solution data and is assigned to $\bar{\nu}_{NN}$ (e) of $Cr(CO)(N_2)_5$. Associated with this $\bar{\nu}_{NN}$ band is the group of matrix-split $\bar{\nu}_{CO}$ bands at ~1921 cm^{-1}, which may, on the basis of the predicted value of 1926 cm^{-1}, be assigned to $\bar{\nu}_{CO}$ (a_1) of $Cr(CO)(N_2)_5$. There is no corresponding band in the solution data, but this is perhaps not surprising in view of the probable weakness of the band compared with the intensities of the bands of the other carbonyl species present in solution. There is also a much weaker $\bar{\nu}_{NN}$ band, which, on the basis of growth and decay studies in the matrix, clearly belongs to the same $Cr(CO)(N_2)_5$ species; it is assigned to $\bar{\nu}_{NN}$ (a_1 low). The third predicted $\bar{\nu}_{NN}$ (a_1 high) is presumably too weak to be observed in these spectra (Table VIA).

$C^{18}O$ enrichment confirms that this molecule contains only one CO group. The results of cocondensation with $C^{16}O$ and with $C^{16}O/C^{18}O$ mixtures are compared in Figure 7. In the $C^{18}O$ experiment there is a new split band (1884 and 1878.1 cm^{-1}) (Table VIB). The shift between the respective components is 42.7 cm^{-1}, which confirms that the original $C^{16}O$ band (Figure 7a) is a matrix-split doublet and also that it arises

Table VII

A. Comparison between Data from Matrix Cocondensation and Liquid-Xe Solution Photochemistry Experiments for $Cr(CO)_2(N_2)_4$

band	$\bar{\nu}$(soln),^{a} cm^{-1}	$I_{\text{obsd}}{}^{d}$	$\bar{\nu}$(matrix),^{b} cm^{-1}	$I_{\text{obsd}}{}^{d}$	approx force field,^{c} cm^{-1}	$I_{\text{pred}}{}^{d}$
a_1 (NN)	2233.5	vw	2242	vw	2234.9	1
a_1 (NN)	2165.0	vw	...	...	2185.9	
b_1 (NN)	2142.4	1	2147	1	2147.8	2
b_2 (NN)	2193.5	0.3	2202	0.3	2190.6	1
a_1 (CO)	1955.4	1	1953	1	1958.5	1
b_1 (CO)	1919.6	1	1916	1	1920.2	1

B. Wavenumbers of $\bar{\nu}_{CO}$ in an N_2 Matrix Doped with a 1:1 Mixture of $C^{16}O/C^{18}O$ for $Cr(CO)_2(N_2)_4$

species	band	$\bar{\nu}_{CO}$	
		obsd^{f}	calcd^{e,g}
cis-$Cr(C^{16}O)_2(N_2)_4$	a_1	1953.4	1953.4
	b_1	1915.8	1915.8
cis-$Cr(C^{16}O)(C^{18}O)(N_2)_4$	a′	1939.1	1941.1
	a′	1883.6	1881.4
cis-$Cr(C^{18}O)_2(N_2)_4$	a_1	1909.3	1906.2
	b_1	1870.3	1869.5

[a] Data from liquid-Xe solution photochemistry (Table IVC).
[b] Data from the matrix cocondensation experiment (Figure 6).
[c] Predicted values from the Timney method (Table IIIB).
[d] Approximate relative intensities, observed and predicted.
[e] $k_{CO} = 1512.1$ N m^{-1}, and $k_{CO,CO} = 29.4$ N m^{-1}. [f] See Figure 8b for spectrum and details of conditions. [g] Mean error 2.03 cm^{-1}.

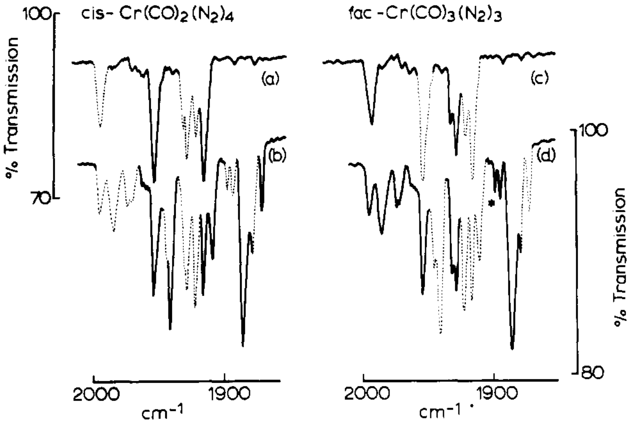

Figure 8. Isotopic substitution for $Cr(CO)_2(N_2)_4$ and $Cr(CO)_3(N_2)_3$. Parts a and c both show the same spectrum obtained by the cocondensation of Cr atoms with an $N_2/C^{16}O$ mixture (100:1) + 40 min of photolysis but have different bands highlighted. In (a) bands marked with a solid line are due to the dicarbonyl $Cr(CO)_2(N_2)_4$. In (c) bands marked with a solid line are due to the tricarbonyl $Cr(CO)_3(N_2)_3$. Similarly, parts b and d both show the same spectrum obtained under conditions identical with those of parts a and c, except that in this case the $C^{16}O$ has been replaced by a 1:1 mixture of $C^{16}O:C^{18}O$. In (b) bands marked with a solid line are due to isotopomers of the *dicarbonyl*, and in (d) these solid bands are due to isotopomers of the *tricarbonyl*. The assignment of the band marked with an asterisk in (d) is doubtful. See Tables VIIB and VIIIB for detailed assignments.

from a molecule containing one CO group.

$Cr(CO)_2(N_2)_4$. Analysis of the growth and decay of band intensities during deposition and subsequent photolysis yields a group of five bands (three $\bar{\nu}_{NN}$ and two $\bar{\nu}_{CO}$), which remain in constant relative intensity. Comparing with the liquid-Xe solution data, we assign these bands to *cis*-$Cr(CO)_2(N_2)_4$ (Table VIIA). Again $C^{18}O$ enrichment is consistent with a species containing two CO groups. On isotopic enrichment, the a_1 and b_1 $\bar{\nu}_{CO}$ bands of *cis*-$Cr(CO)_2(N_2)_4$ each give rise to a 1:2:1 triplet. These triplets are readily identified (Figure 8b), and the observed frequencies along with those calculated by employing a frequency-factored force field are shown in Table VIIB.

Table VIII

A. Comparison between Data from Matrix Cocondensation and Liquid-Xe Solution Photochemistry Experiments for $Cr(CO)_3(N_2)_3$

band	$\bar{\nu}$(soln),^{a} cm^{-1}	$I_{\text{obsd}}{}^{d}$	$\bar{\nu}$(matrix),^{b} cm^{-1}	$I_{\text{obsd}}{}^{d}$	approx force field,^{c} cm^{-1}	$I_{\text{pred}}{}^{d}$
		fac-$Cr(CO)_3(N_2)_3$				
a_1 (NN)	2241.3	0.8	2247	vw	2238	1
e (NN)	2207.2	2	2218	vw	2202	2
a_1 (CO)	1994.6	1.4	1995	1	1990.2	1
e (CO)	1931.8	2	1928/ 1932^{e}	2	1933.4	2
		mer-$Cr(CO)_3(N_2)_3$				
a_1 (NN)	2233.5	vw	...		2232.8	1
a_1 (NN)	2186.3	0.2	...		2198.6	
b_1 (NN)	2159.3	2	2164		2159.4	2
a_1 (CO)	2023.0	vw	...		2023.4	1
b_2 (CO)	1947.2	0.3	1948		1948.8	2

B. Wavenumbers of $\bar{\nu}_{CO}$ in an N_2 Matrix Doped with a 1:1 Mixture of $C^{16}O/C^{18}O$ for $Cr(CO)_3(N_2)_3$

species	band	$\bar{\nu}_{CO}$, cm^{-1}	
		obsd^{g}	calcd^{f,i}
$Cr(C^{16}O)_3(N_2)_3$	a_1	1994.9	1995.2
	e	1927.9	1927.1
$Cr(C^{16}O)_2(C^{18}O)(N_2)_3$	a′	1983.3	1985.2
	a′	1893.1	1893.7
	a″	1927.9	1927.1
$Cr(C^{16}O)(C^{18}O)_2(N_2)_3$	a′	1972.3	1972.6
	a′	(1897.6)^{h}	1905.7
	a″	1883.6	1884.3
$Cr(C^{18}O)_3(N_2)_3$	a_1	1953.4	1950.8
	e	1883.6	1884.3

[a] Data from liquid-Xe solution photochemistry (Table IVB).
[b] Data from the matrix cocondensation experiment (Figure 6).
[c] Predicted values from the Timney method (Table IIIB).
[d] Approximate relative intensities, observed and predicted.
[e] Matrix-split group. [f] $k_{CO} = 1536.2$ N m^{-1}, and $k_{CO,CO} = 36.0$ N m^{-1}. [g] See Figure 8d for spectrum and details of conditions. [h] Doubtful assignment; see text for discussion.
[i] Mean error (excluding 1897.6-cm^{-1} band) 0.97 cm^{-1}.

There are no bands in the cocondensation experiments that can be assigned to *trans*-$Cr(CO)_2(N_2)_4$. It is possible that no *trans*-$Cr(CO)_2(N_2)_4$ was formed, but more probably, the bands are masked by those of the cis isomer, particularly since both IR-active bands of the trans isomer are predicted to coincide with absorptions of the *cis*-dicarbonyl or *fac*-tricarbonyl isomers (q.v. Table IIIB).

$Cr(CO)_3(N_2)_3$. As with the previous $Cr(CO)_{6-x}(N_2)_x$ species, we can pick out bands with constant relative intensities assignable to both the *mer* and the *fac* isomers of $Cr(CO)_3(N_2)_3$ (Table VIIIA). Unfortunately, only two of the five solution IR bands of the *mer* isomer are observed in the matrix, presumably because of weakness and general overlap. With $C^{18}O$ enrichment (Figure 8d), it can be seen that the whole spectrum is somewhat congested (by the presence of $Cr(CO)_2(N_2)_4$ species), but nevertheless one can tentatively assign eight bands to isotopomers of $Cr(CO)_3(N_2)_3$, albeit with two bands overlapping those of $Cr(CO)_2(N_2)_4$. Eight $\bar{\nu}_{CO}$ bands would be predicted for the $C^{18}O$-enriched *fac* isomer of $Cr(CO)_3(N_2)_3$. Table VIIIB shows the best attempt to fit the frequencies of these bands with use of a frequency-factored force field. The attempt is less than successful, perhaps due to $\bar{\nu}_{NN}/\bar{\nu}_{CO}$ coupling. Figure 8 clearly illustrates the problems in analyzing isotopic spectra of matrices containing several

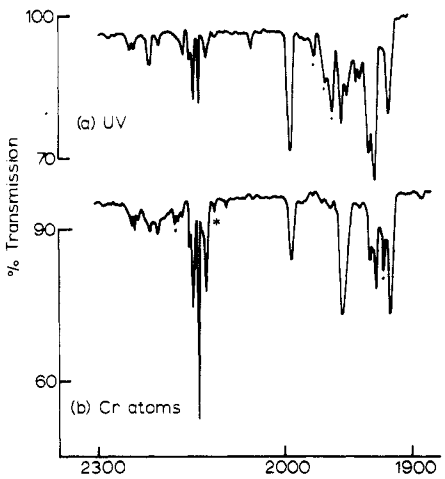

Figure 9. Comparison between matrix cocondensation and matrix photochemistry experiments: (a) (UV photolysis) IR spectrum following photolysis of $Cr(CO)_6$ in a pure nitrogen matrix at 17 K (bands marked with a dot are assigned to $Cr(CO)_5N_2$ and $Cr(CO)_4(N_2)_2$; these bands do not appear in the cocondensation spectrum); (b) (Cr atom cocondensation) IR spectrum of matrix resulting from cocondensation of chromium atoms with a 100:1 mixture of N_2 and $C^{16}O$ (the band marked with an asterisk at 2112 cm^{-1} is assigned to $Cr(N_2)_6$; other bands in the spectrum, marked with a dot, which do not appear in (a), are due to $Cr(CO)(N_2)_5$). See Table IX for band positions and assignments.

Table IX. Comparison between Data for Matrix Photochemistry and Matrix Cocondensation Experiments

		$\bar{\nu}_{CO}/\bar{\nu}_{NN}$, cm^{-1}	
species	band	matrix photochem[a]	matrix cocond[b]
$Cr(CO)(N_2)_5$	e (NN)	2128	2127
cis-$Cr(CO)_2(N_2)_4$	b_2 (NN)	2202	2202
	b_1 (NN)	2147	2147
	a_1 (CO)	1953	1953
	b_1 (CO)	1915	1916
fac-$Cr(CO)_3(N_2)_3$	a_1 (NN)	2247	2247
	e (NN)	2217	2218
	a_1 (CO)	1994	1995
	e (CO)	1927.6/1930.9[c]	1927.9/1931.8[c]
mer-$Cr(CO)_3(N_2)_3$	b_1 (NN)	2164	2164
	b_2 (CO)	1948	~1948 sh

[a] See Figure 9a for details of conditions. [b] See Figure 9b for details of conditions. [c] Matrix-split doublet.

species, and so the poor numerical fit is not very surprising.

Thus, the matrix cocondensation experiments generally support our assignments of bands in liquid-Xe solutions. They do not, however, preclude the possibility that some of the species, both in the matrix and in solution, are polynuclear, i.e. contain more than one chromium atom. Fortunately, this possibility can be eliminated by photolysis of matrix-isolated $Cr(CO)_6$.

Matrix Photochemistry. Previous photolysis experiments with $Cr(CO)_6$ in various matrices have shown that polynuclear species are only formed in appreciable amounts in concentrated matrices.[25] Thus, if photolysis of $Cr(CO)_6$ isolated in dilute matrices were to produce IR bands at the same frequencies as those in the $Cr/CO/N_2$ cocondensation experiments, it would be reasonable to assume that the $Cr_y(CO)_{6-x}(N_2)_x$ species in the matrix (and hence in liquid-Xe solution) were all mononuclear (i.e., $y = 1$). Figure 9 compares spectra produced by photolysis[13] and cocondensation.[13] With hindsight, it is relatively simple to see how the bands correlate, and the frequencies of the bands are virtually identical (Table IX). Thus, our assignment of the bands to mononuclear species is vindicated. It must be stressed that, although the band assignment now appears possible, this is only because the liquid-Xe experiments and Timney's approximations have made it so.

Table X. Thermal Stabilities[a] of Molecules in the Series $Cr(CO)_{6-x}(N_2)_x$

$Cr(CO)_5N_2$	stable at −35 °C
$Cr(CO)_4(N_2)_2$	$t_{1/2}$ = 10 min at −55 °C
$Cr(CO)_3(N_2)_3$	$t_{1/2}$ = 15 min at −79 °C
$Cr(CO)_2(N_2)_4$	much less stable but detectable at or below −79 °C
$Cr(CO)(N_2)_5$	

[a] Thermal stability was assessed by warming the liquid-Xe solution to the temperature indicated and monitoring the stability of the species present by scanning the IR spectrum in the relevant region at approximately 3-min intervals (see Figure 4, for example).

VI. Conclusions

An examination of the growth and decay behavior of the IR absorptions observed when $Cr(CO)_6$ is photolyzed in solution in a Xe/N_2 mixture (~1% N_2), combined with simple intensity and force field arguments, allows us to unravel almost completely a complex photochemical problem in identifying and assigning vibrational frequencies to the series of molecules $Cr(CO)_{6-x}(N_2)_x$. The problem becomes more difficult the greater the degree of N_2 substitution because both the thermal stability and the intensity of the IR absorptions of the complexes decrease (Table X). Somewhat disappointingly, we found no evidence in these solution experiments for any band that could be assigned unambiguously to the completely substituted species $Cr(N_2)_6$, which is presumably too unstable in liquid Xe at −79 °C. This instability is not very surprising as $Cr(CO)(N_2)_5$ already contains 63% nitrogen by weight. Experiments at lower temperatuers and in liquid Kr were attempted, but the decreasing solubility of both $Cr(CO)_6$ and presumably its products as the temperature is reduced leads to the appearance of only weak product bands.

This situation is in contrast to that in previous matrix experiments designed to generate this series of molecules, where the IR spectra were extremely complex and unyielding. However, with the benefit of hindsight and by comparison with the present solution data it has been possible to interpret the matrix data and thereby add further weight to our assignments in the solution experiments.

Acknowledgment. We thank the SERC for support and for a Senior Visiting Fellowship (to W.B.M.). We are particularly grateful to Mr. R. Howsely for his contribution[22] to this work, and to Mr. J. G. McLaughlin for his untiring assistance. Thanks are also due to Mr. K. W. Rigley and his colleagues in the Chemistry Department Workshop at Nottingham for assistance in setting up the equipment for the low-temperature solution experiments. In addition the generous loan of a Lambda 5 UV/Vis spectrometer by Perkin-Elmer Ltd. is gratefully acknowledged. We have also enjoyed fruitful discussion with Dr. A. J. Downs and Mr. M. Hawkins.

Registry No. $Cr(CO)_6$, 13007-92-6; $Cr(CO)_5(N_2)$, 34416-63-2; *cis*-$Cr(CO)_4(N_2)_2$, 84130-32-5; *trans*-$Cr(CO)_4(N_2)_2$, 84172-83-8; *fac*-$Cr(CO)_3(N_2)_3$, 84234-87-7; *mer*-$Cr(CO)_3(N_2)_3$, 84130-33-6; *cis*-$Cr(CO)_2(N_2)_4$, 84172-84-9; *trans*-$Cr(CO)_2(N_2)_4$, 84130-35-8; $Cr(CO)(N_2)_5$, 84130-34-7.

---

(25) Burdett, J. K.; Graham, M. A.; Perutz, R. N.; Poliakoff, M.; Rest, A. J.; Turner, J. J.; Turner, R. F. *J. Am. Chem. Soc.* **1975**, *97*, 4805.